Supporting information

Proteomic profile of hard corona of charged polystyrene nanoparticles exposed to sea urchin *Paracentrotus lividus* coelomic fluid highlights potential drivers of toxicity

Giacomo Grassi[a]*, Claudia Landi[b], Camilla della Torre[c], Elisa Bergami[a], Luca Bini[b] and Ilaria Corsi[a].

[a]Department of Physical, Earth and Environmental Sciences, University of Siena, 53100 Siena, Italy

[b]Department of Life Sciences, University of Siena, 53100 Siena, Italy

[c]Department of Life Sciences, University of Milan, 20133 Milan, Italy

*Corresponding author, Phone: +39 0577 232811; email: grassi23@student.unisi.it

Number of pages: 8

Number of tables: 2

Number of figures: 1

Table of contents:

Table S1. Chemical parameters including heavy metals (Cr, As, Cd, Hg, Pb) of natural sea water samples used in the study for the maintenance of *P. lividus* organism ins aquaria and for PS NPs characterization. Data also available free of charge at: SIRA RSS. www.sira.arpat.toscana.it/.

Parameter	
Total Oxygen	8.08 mg/L
N_{TOT}	0.0406 mg/L
P_{TOT}	< 0.0124 mg/L
Salinity	38‰
Cr_{TOT}	< 1 µg/L
Cr_{VI}	< 0.5 µg/L
As	1.3 µg/L
Ni	< 1 µg/L
Cd	< 0.05 µg/L
Hg	< 0.01 µg/L
Pb	< 1 µg/L
Hydrocarbons (C10 – C40)	< 100 µg/L

Additional description of methods

Polystyrene NPs characterization. CF was thawed, centrifuged for 5 min at 16000×*g* to eliminate possible protein aggregates and used for PS-NH_2 and PS-COOH dispersions, at a concentration of 25 µg mL^{-1}. Dispersion parameters were analyzed by dynamic light scattering (DLS), on a Malvern Zetasizer ZS (Malvern Instruments, Worchestershire, UK), with a 633 nm laser beam and a backscattering angle of 90°. NPs size distribution, mean hydrodynamic diameter (Z-average) and polydispersity index (PdI) were obtained at 18°C, with three independent measurements, each consisting of 11 sub-runs. The zeta potential values were acquired as triplicate measurements, each consisting of several runs, the number of which was determined instrumentally (max. 100 runs) until a reliable measurement was obtained. The influence of CF on PS NPs surface charge was investigated by measuring the ζ-potential through electrophoretic light scattering. The contribution of proteins or protein aggregates present in CF was negligible and did not affect light scattering measurements.

Preparation and desorption of protein coronas. The native protein concentration of coelomic fluid was in the range of 300 to 500 µg mL^{-1}. Therefore, CF had to be additionally processed prior

PS-NPs incubations. Briefly, the CF was thawed and transferred to Amicon Ultra-15 (Millipore) centrifugal filter units with a 3 kDa MWCO regenerated cellulose membranes and centrifuged at 3500×*g*, 4°C, until the desired volume was achieved (5 mg mL^{-1} average protein content). The concentrated CF was centrifuged at 16000×*g*, for 10 min at 4°C to remove possible protein aggregates, if any, before incubation with PS-NH_2 and PS-COOH NPs. Following incubation the protein-particle complexes were washed three times by centrifugation at 18000×g, at 18°C for 15 min and resuspension in PBS. NP-corona pellet was recovered and hardly retained proteins were eluted from the washed NP-corona complexes with a methanol/chloroform precipitation procedure[1,2], with minor modifications. Initially, 400 µL of methanol were added to the washed NPs-corona pellet, which was fully resuspended by a brief pulse (5 s) of bath sonication. The PS NPs were then dissolved with the addition of 200 µL of chloroform followed by 5 s of bath sonication, thus breaking down the core polymeric structure of NPs and releasing proteins from the NP surface, maximizing the yield. The desorbed proteins were the precipitated by the addition of 300 µL of demineralized water and centrifugation at 9000×g for 1 min. A triphasic system was formed and the corona proteins, located at the interface, where recovered by removing the upper water-methanol layer and pelleted by addition of 400 µL of methanol, vigorous vortexing and centrifugation at 12000×*g* for 5 min. The obtained pellet was air-dried for 10 min and rehydrated in 150 µL of Bio-Rad Protein Solubilization Buffer (urea, thiourea, CHAPS and NDSB-201), supplemented with 1% DTT as a reducing agent. Finally, the samples were quantitated with 2-D QuantKit® (GE healthcare) for total protein concentration and diluted, when necessary, to 6 µg $µL^{-1}$, prior adding 2% (v/v) carrier ampholytes (pH 3-10).

Proteomic analysis. Isoelectric focusing (IEF) was carried out on nonlinear wide-range immobilized pH gradients (pH 3.0–10; 18 cm long IPG strips; GE Healthcare, Uppsala, Sweden) and achieved using an EttanIPGphor™ system (GE Healthcare). Six hundred micrograms of total protein were loaded by rehydration loading, overnight at 30 V. After rehydration step, first dimensional run was carried out at 16°C under the following electrical conditions: 200 V for 8 h, a gradient until 3500 V for 2 h, a step of 3500 V for other 2 h. After that, a gradient until 5000V for 2 h is applied and maintained 5000 V for other 3 h, another gradient until 8000 V for 1 h and a step of 8000 V for 3 h. At the end a gradient until 10000 V for 1 h is performed and maintained for a total of 100,000 Vh. After the first dimensional run, the IPG gels were equilibrated in 6 M urea, 2 % w/v SDS, 2 % w/v DTE, 3 0% v/v glycerol and 0.05 M Tris-HCl pH 6.8 for 12 min and for a further 5 min in the same solution where DTE was replaced by 2.5 % w/v iodoacetamide and a trace of bromophenol blue. After the two equilibration steps, second dimensional separation was carried out at 15°C on 9-16 % home-made polyacrylamide linear gradient gels (18 × 20 cm × 1.5 mm) at 17

W/gel using an EttanDalt II system (GE Healthcare). Runs were performed until the dye front reached the bottom of the gel. MS-preparatory gels were stained with SYPRO Ruby (Bio-rad headquarters, Hercules, California) according to the manufacturer's instructions. Bind-silane (γ-methacryloxypropyltrimethoxysilane) (LKBProdukter AB, Brommo, Sweden) was used to attach polyacrylamide gels covalently to a glass surface. Preparative gel images stained with SYPRO Ruby were digitized with a Typhoon 9400 laser densitometer (GE Healthcare). Computer-aided 2D image was carried out with the Image Master Platinum 7.0 computer system (GE Healthcare). The significant variations of proteins were investigated by comparing gels from CF and PS-NH_2 and PS-COOH corona. Spots corresponding to differentially abundant proteins were statistically evaluated in terms of the mean relative volume (vol. %) using Student's t-test for unpaired samples. The significance level was defined as $p < 0.05$. A minimum 2-folds change cut-off relative to different samples was employed as a further criterion for differential abundance.

Protein Identification by Mass Spectrometry. In order to perform protein identification of the principal spots present in the gels, the well visible spots were selected by a landmark and mechanically excised from the gel. Protein identification was carried out by peptide mass fingerprinting (PMF) on an ultrafleXtreme™ MALDI-ToF/ToF instrument (Bruker Corporation, Billerica, MA, United States). After visualization using a SYPRO Ruby staining protocol, all the spots of interest were mechanically excised with an Ettan Spot Picker (GE Healthcare), destained in 2.5 mM ammonium bicarbonate and 50% acetonitrile and finally, dehydrated in acetonitrile. They were then re-hydrated in trypsin solution and an in-gel protein digestion was performed overnight with incubation at 37°C. Each protein digest (0.75 µl) was spotted onto a MALDI target and allowed to air dry. Then 0.75 µl of matrix solution (saturated solution of α-cyano-4-hydroxycinnamic acid in 50 % (v/v) acetonitrile and 0.5 % (v/v) TFA) was applied to the sample and dried again. MS analysis was then performed with UltrafleXtreme™ MALDI-ToF/ToF instrument (Bruker Corporation, Billerica, MA, United States) equipped with a 200 Hz smartbeam™ I laser in the positive reflector mode according to defined parameters: 80 ns of delay; ion source 1: 25 kV; ion source 2: 21.75 kV; lens voltage: 9.50 kV; reflector voltage: 26.30 kV; and reflector 2 voltage: 14.00 kV. The applied laser wavelength and frequency were 353 nm and 100 Hz, respectively, and the percentage was set to 46%. Final mass spectra were produced by averaging 1500 laser shots targeting five different position within the spot. Spectra were acquired automatically and the Flex Analysis software version 3.0 (Bruker) was used for their analysis and for the assignment of the peaks. The applied software generated a list of peaks up to 200, using a signal-to-noise ratio of 3 as threshold for peak acceptance. Recorded spectra were calibrated using

peptides arising from trypsin autoproteolysis as internal standard. The resulting mass lists were filtered for contaminant removal: mass matrix-related ions, trypsin auto-lysis and keratin peaks. PMF searches were carried out against the NCBIprot/SwissProt databases using MASCOT search engine available on-line (Matrix Science Ltd, London, UK, http://www.matrixscience.com). Taxonomy was limited to Metazoa, a mass tolerance of 100 ppm was allowed and the number of accepted missed cleavage sites was set at one. Alkylation of cysteine by carbamidomethylation was considered as a fixed modification, while oxidation of methionine was considered as a variable modification. The criteria used to accept identifications included the extent of sequence coverage, the number of matched peptides and the MASCOT algorithm assigned a probabilistic score (> 80 or $p < 0.001$).

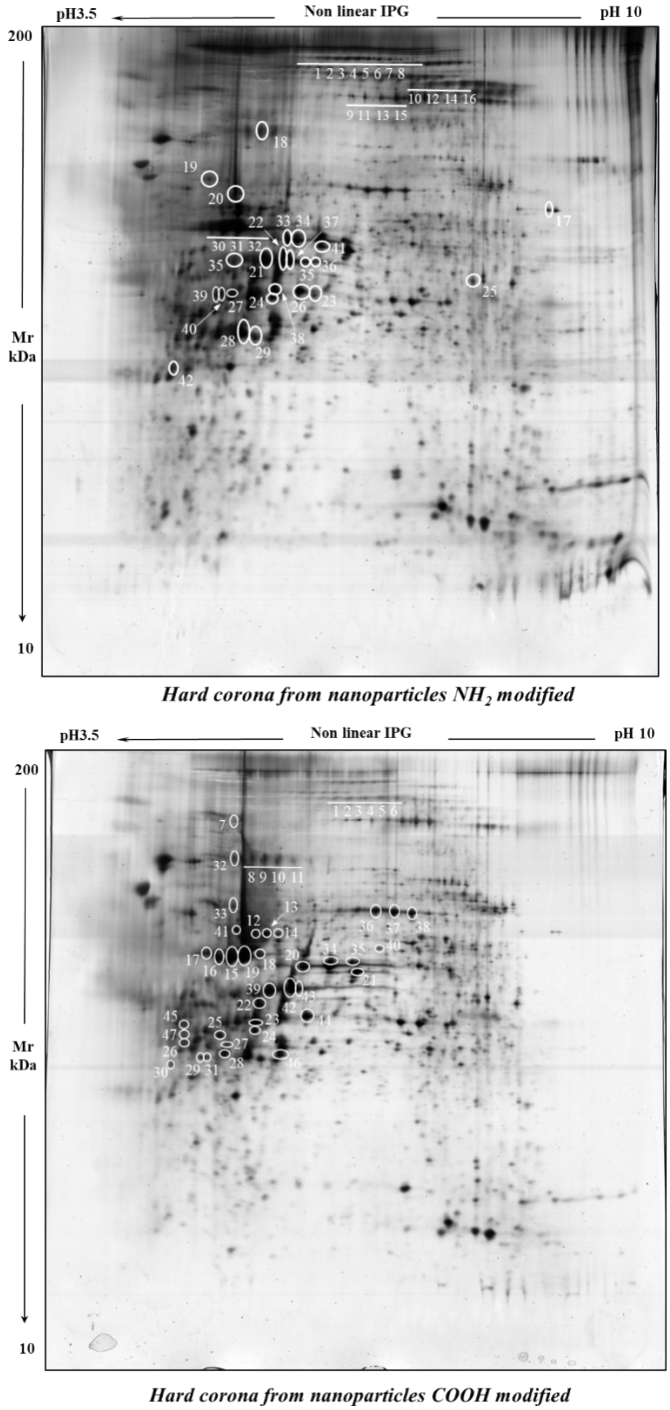

Figure S1. 2DE gels of protein coronas from PS-NH_2 (upper panel) and PS-COOH (lower panel) NPs. Spots circled and numbered have been excised for tryptic digestion and MALDI-TOF identification.

Table S2. List of identified proteins from PS-COOH NPs hard corona

Spot number	Name	Accession number	Species	p/ MW	Mascot Search Results		
					Score	Coverage	Matched peptides
1	Toposome	AAQ17121.1	Paracentrotus lividus	6.15 155336	111	10	14
2	Toposome	AAQ17121.2	Paracentrotus lividus	6.15 155337	147	9	13
3	Toposome	AAQ17121.1	Paracentrotus lividus	6.15 155336	103	9	11
4	Toposome	AAQ17121.1	Paracentrotus lividus	6.15 155336	114	12	18
5	Toposome	AAQ17121.1	Paracentrotus lividus	6.15 155336	108	13	18
6	Toposome	AAQ17121.1	Paracentrotus lividus	6.15 155337	111	10	10
7	Nectin Precursor	CAE17512.2	Paracentrotus lividus	6.02 108817	134	21	14
8	Actin, cytoskeletal 2A	Q07903	Strongylocentrotus purpuratus	5.29 42059	120	40	12
9	Actin, cytoskeletal 2B	P69005	Strongylocentrotus purpuratus	5.29 42056	112	39	11
10	Actin, cytoskeletal 2B	P69005	Strongylocentrotus purpuratus	5.29 42056	113	39	12
11	actin, cytoskeletal 2B	NP_999693.1	Strongylocentrotus purpuratus	5.29 42057	138	35	12
12	actin, cytoskeletal 2B	NP_999693.1	Strongylocentrotus purpuratus	5.29 42057	103	39	12
13	actin, cytoskeletal 2B	NP_999693.1	Strongylocentrotus purpuratus	5.29 42057	161	48	16
14	actin, cytoskeletal 2B	NP_999693.1	Strongylocentrotus purpuratus	5.29 42057	168	40	14
15	actin, cytoskeletal 2B	NP_999693.1	Strongylocentrotus purpuratus	5.29 42057	216	50	21
16	actin, cytoskeletal 2B	NP_999693.1	Strongylocentrotus purpuratus	5.29 42057	178	44	16
17	actin, cytoskeletal 2B	NP_999693.1	Strongylocentrotus purpuratus	5.29 42057	123	28	11
18	actin, cytoskeletal 2B	NP_999693.1	Strongylocentrotus purpuratus	5.29 42057	179	41	15
19	actin, cytoskeletal 2B	NP_999693.1	Strongylocentrotus purpuratus	5.29 42057	185	44	18
20	actin, cytoskeletal 2B	NP_999693.1	Strongylocentrotus purpuratus	5.29 42057	107	35	13
21	actin, cytoskeletal 2B	NP_999693.1	Strongylocentrotus purpuratus	5.29 42057	171	42	17
22	actin, cytoskeletal 2B	NP_999693.1	Strongylocentrotus purpuratus	5.29 42057	138	38	11
23	actin, cytoskeletal 2B	NP_999693.1	Strongylocentrotus purpuratus	5.29 42057	153	41	12
24	actin, cytoskeletal 2B	NP_999693.1	Strongylocentrotus purpuratus	5.29 42057	138	35	12
25	actin, cytoskeletal 2B	NP_999693.1	Strongylocentrotus purpuratus	5.29 42057	119	35	10
26	actin, cytoskeletal 2B	NP_999693.1	Strongylocentrotus purpuratus	5.29 42057	97	37	9
27	actin, cytoskeletal 2B	NP_999693.1	Strongylocentrotus purpuratus	5.29 42057	159	45	16
28	actin, cytoskeletal 2B	NP_999693.1	Strongylocentrotus purpuratus	5.29 42057	123	34	11
29	actin, cytoskeletal 2B	NP_999693.1	Strongylocentrotus purpuratus	5.29 42057	107	37	10
30	actin, cytoskeletal 2B	NP_999693.1	Strongylocentrotus purpuratus	5.29 42057	87	31	8
31	actin, cytoskeletal 2B	NP_999693.1	Strongylocentrotus purpuratus	5.29 42057	96	31	8
32	actin, cytoskeletal 3B	NP_999692.1	Strongylocentrotus purpuratus	5.22 42147	90	33	9
33	actin, cytoskeletal 3B	NP_999692.1	Strongylocentrotus purpuratus	5.22 42147	110	22	8
34	actin, cytoskeletal 3B	XP_003725373	Strongylocentrotus purpuratus	5.2242062	153	41	15
	actin, cytoskeletal 2B	NP_999693.1	Strongylocentrotus purpuratus	5.29 42057	153	41	15
35	actin, cytoskeletal 3B	XP_003725373	Strongylocentrotus purpuratus	5.2242062	205	54	20
	actin, cytoskeletal 2B	NP_999693.1	Strongylocentrotus purpuratus	5.29 42057	205	54	20
36	fascin	NP_999701.1	Strongylocentrotus purpuratus	5.46 55537	109	18	11
37	fascin	NP_999701.1/Q05634	Strongylocentrotus purpuratus	5.46 55537	118	21	11
38	fascin	NP_999701.1	Strongylocentrotus purpuratus	5.46 55537	102	15	9
39	actin-15B	XP_001176242.1	Strongylocentrotus purpuratus	5.29 42059	91	42	11
40	actin-15B	XP_001176242.1	Strongylocentrotus purpuratus	5.29 42059	106	30	8
41	actin-15B	XP_001176242.1	Strongylocentrotus purpuratus	5.29 42059	131	37	10
42	actin-15B	XP_001176242.1	Strongylocentrotus purpuratus	5.29 42059	153	40	12
43	actin-15B	XP_001176242.1	Strongylocentrotus purpuratus	5.29 42059	106	33	9
44	actin-15B	XP_001176242.1	Strongylocentrotus purpuratus	5.29 42059	89	33	8
45	actin-15B	XP_001176242.1	Strongylocentrotus purpuratus	5.29 42059	108	28	7
46	actin-15B	XP_001176242.1	Strongylocentrotus purpuratus	5.29 42059	118	30	10
47	Muscle actin isoform X1	XP_011661664.1	Strongylocentrotus purpuratus	5.30 42077	92	33	8

Table S3. Table of identified proteins from PS-NH_2 NPs hard coronas

Spot number	Name	Accession number	Species	p/ MW	Mascot Search Results		
					Score	Coverage	Matched peptides
1	Toposome	AAQ17121.1	Paracentrotus lividus	6.15 155336	194	13	17
2	Toposome	AAQ17121.2	Paracentrotus lividus	6.15 155337	96	7	10
3	Toposome	AAQ17121.1	Paracentrotus lividus	6.15 155336	163	12	16
4	Toposome	AAQ17121.1	Paracentrotus lividus	6.15 155336	205	16	21
5	Toposome	AAQ17121.1	Paracentrotus lividus	6.15 155336	114	8	11
6	Toposome	AAQ17121.1	Paracentrotus lividus	6.15 155337	113	11	15
7	Toposome	AAQ17121.1	Paracentrotus lividus	6.15 155337	180	15	18
8	Toposome	AAQ17121.1	Paracentrotus lividus	6.15 155336	184	14	17
9	nectin precursor	CAE17512.2	Paracentrotus lividus	6.02 108817	170	20	18
10	nectin variant 2 precursor	ALY05410.1	Paracentrotus lividus	5.95 108911	111	14	14
11	nectin precursor	CAE17512.2	Paracentrotus lividus	6.02 108817	141	21	18
12	nectin variant 2 precursor	ALY05410.1	Paracentrotus lividus	5.95 108911	104	17	15
13	nectin precursor	CAE17512.2	Paracentrotus lividus	6.02 108817	170	29	21
14	nectin variant 2 precursor	ALY05410.1	Paracentrotus lividus	5.95 108911	120	23	17
15	nectin precursor	CAE17512.2	Paracentrotus lividus	6.02 108817	133	21	18
16	nectin variant 2 precursor	ALY05410.1	Paracentrotus lividus	5.95 108911	110	20	16
17	flotillin-1	XP_791741.2	Strongylocentrotus purpuratus	7.57 47559	122	31	12
18	Actin, cytoskeletal 2A	W4Y1A3	Strongylocentrotus purpuratus	5.29 42059	112	31	10
19	actin, cytoskeletal 2B	NP_999693.1	Strongylocentrotus purpuratus	5.29 42057	168	32	16
20	actin, cytoskeletal 2B	NP_999693.1	Strongylocentrotus purpuratus	5.29 42057	148	51	16
21	actin, cytoskeletal 2B	NP_999693.1	Strongylocentrotus purpuratus	5.29 42057	148	33	13
22	actin, cytoskeletal 2B	NP_999693.1	Strongylocentrotus purpuratus	5.29 42057	166	41	15
23	actin, cytoskeletal 2B	NP_999693.1	Strongylocentrotus purpuratus	5.29 42057	109	35	11
24	actin, cytoskeletal 2B	NP_999693.1	Strongylocentrotus purpuratus	5.29 42057	143	32	14
25	actin, cytoskeletal 2B	NP_999693.1	Strongylocentrotus purpuratus	5.29 42057	155	35	16
26	actin, cytoskeletal 2B	NP_999693.1	Strongylocentrotus purpuratus	5.29 42057	161	41	18
27	actin, cytoskeletal 2B	NP_999693.1	Strongylocentrotus purpuratus	5.29 42057	144	34	15
28	actin, cytoskeletal 2B	NP_999693.1	Strongylocentrotus purpuratus	5.29 42057	150	29	16
29	actin, cytoskeletal 2B	NP_999693.1	Strongylocentrotus purpuratus	5.29 42057	120	33	14
30	muscle actin isoform X1	XP_011661664.1	Strongylocentrotus purpuratus	5.30 42077	147	38	13
31	muscle actin isoform X1	XP_011661664.1	Strongylocentrotus purpuratus	5.30 42077	157	46	15
32	muscle actin isoform X1	XP_011661664.1	Strongylocentrotus purpuratus	5.30 42077	161	42	15
33	actin-15B	XP_001176242.1	Strongylocentrotus purpuratus	5.29 42059	158	36	14
34	actin-15B	XP_001176242.1	Strongylocentrotus purpuratus	5.29 42059	130	32	12
35	actin-15B	XP_001176242.1	Strongylocentrotus purpuratus	5.29 42059	147	36	13
36	actin-15B	XP_001176242.1	Strongylocentrotus purpuratus	5.29 42059	130	35	13
37	actin-15B	XP_001176242.1	Strongylocentrotus purpuratus	5.29 42059	154	39	17
38	actin-15B	XP_001176242.1	Strongylocentrotus purpuratus	5.29 42059	203	40	16
39	actin-15B	XP_001176242.1	Strongylocentrotus purpuratus	5.29 42059	121	32	14
40	actin-15B	XP_001176242.1	Strongylocentrotus purpuratus	5.29 42059	112	31	10
41	guanine nucleotide-binding protein subunit beta	XP_001176793.1	Strongylocentrotus purpuratus	5.79 38221	135	43	15
42	actin related protein 1	NP_999634.1	Strongylocentrotus purpuratus	5.29 42146	184	33	15

References

1 D. Wessel and U. I. Flügge, A method for the quantitative recovery of protein in dilute solution in the presence of detergents and lipids, *Anal. Biochem.*, 1984, **138**, 141–143.

2 S. Ritz, S. Schöttler, N. Kotman, G. Baier, A. Musyanovych, J. Kuharev, K. Landfester, H. Schild, O. Jahn, S. Tenzer and V. Mailänder, Protein Corona of Nanoparticles: Distinct Proteins Regulate the Cellular Uptake, *Biomacromolecules*, 2015, **16**, 1311–1321.